Revista Brasileira de Cartografia
ISSN 1808-0936 | https://doi.org/10.14393/revbrascartogr
Sociedade Brasileira de Cartografia, Geodésia, Fotogrametria e Sensoriamento Remoto

Towards a Robust Approach for Multitemporal Landcover Dataset: 3 Decades of Landcover Changes in Piauí, Brazil

Rumo à uma Abordagem Robusta para um Conjunto de Dados de Cobertura Vegetal Multitemporal: 3 Décadas de Mudanças no Piauí, Brasil

Danilo de Sousa Lopes [1], Rodrigo Affonso de Albuquerque Nóbrega [2] e Diego Rodrigues Macedo [3]

1 Universidade Federal de Minas Gerais, Instituto de Geociências, Programa de Pós-graduação em Análise e Modelagem de Sistemas Ambientais, Belo Horizonte, Brazil. danilolopesgeo@gmail.com.
ORCID: https://orcid.org/0000-0002-7082-7236

2 Universidade Federal de Minas Gerais, Instituto de Geociências, Departamento de Cartografia, Belo Horizonte, Brazil. raanobrega@ufmg.br.
ORCID: https://orcid.org/0000-0001-7058-5903

3 Universidade Federal de Minas Gerais, Instituto de Geociências, Departamento de Geografia, Belo Horizonte, Brazil. diegorm@ufmg.br.
ORCID: https://orcid.org/0000-0002-1178-4969

Recebido: 08.2021 | Aceito: 12.2021

Abstract: Mapping the changes of land use and cover through the classification of satellite images is one of the essential sources to investigate and monitor the Earth´s surface. When performed in a multitemporal perspective, this approach requires specific procedures to match the images used. Considering that parkland/grassland savanna patches could increase over time due to different uses, this research aims to present a suitable method for processing Landsat-like images to investigate land cover dynamics. The study area covers seven municipalities in the Brazilian state of Piauí, Cerrado biome, which has been substantially affected by deforestation due to extensive agricultural projects in the past decades. The semi-automatic satellite imaging georegistration and the object-oriented classification of Landsat 5 and 8 satellites over the last 30 years in decadal periods are among the methodological procedures used. Findings demonstrate the semi-automatic image registration process as an effective method for the geometric correction of Landsat scenes, and the object-based classification procedures are appropriate for multitemporal studies allowing comparative metrics of landcover class changes by period. Regarding the remaining natural landcover within the study area, the results showed a substantial decrease of woodland savanna patches from 73% in 1986 to 43% in 2016, while agricultural fields increased from 4% to 25% in 30 years.
Keywords: Automatic Image Registration. OBIA. Multitemporal analysis. Cerrado. Landcover change.

Resumo: Mapear as mudanças de uso e cobertura da terra por meio da classificação de imagens de satélite é uma das fontes mais importantes para investigar e monitorar a superfície terrestre. Essas abordagens, quando realizadas em uma perspectiva multitemporal, requerem procedimentos específicos para coincidir com as imagens utilizadas. Considerando que fragmentos de Cerrado podem aumentar ao longo do tempo devido a diferentes usos, esta pesquisa visa um método adequado de processamento de imagens Landsat para investigar a dinâmica do uso da terra. A área de estudo cobre sete cidades do estado do Piauí, bioma Cerrado, uma área que tem sido afetada por grandes desmatamentos devido a projetos agrícolas. Dentre os procedimentos metodológicos utilizados estão as técnicas de georreferenciamento semiautomático da coleção de imagens orbitais e a classificação orientada a objetos, ambas aplicadas a dados dos satélites Landsat 5 e 8 nos últimos 30 anos em períodos decenais. Com os resultados obtidos, fica evidente que o processo de registro semiautomático de imagens é um método eficaz para a correção geométrica de cenas Landsat e que procedimentos de classificação baseados em objetos, baseados nesta metodologia, são adequados para estudos multitemporais, possibilitando o cálculo de métricas comparativas de mudanças nas classes de cobertura da terra por período. Os resultados mostraram que as manchas de savana florestal diminuíram de 73% em 1986 para 43% em 2016, enquanto os campos agrícolas aumentaram de 4% para 25% em 30 anos.
Palavras-chave: Registro Automático de Imagens. OBIA. Análise Multitemporal. Cerrado. Mudança da cobertura da terra.

1 INTRODUCTION

Over the last three decades, the Cerrado (Brazilian Savanna biome) has been an alternative to the deforestation in the Amazon, and the most intense exploration of this region is drove either by agricultural and pasture expansion or by forest plantations (AGUIAR; MONTEIRO, 2005; STRASSBURG et al., 2017). The state of Piauí is located within a transition between the biomes Caatinga at east and Cerrado at the west, where the new grain-oriented agriculture is pushing the economy and driving significant landscape changes. As for the governance policies, between the 1970s and 1980s, the region experienced the implantation of agricultural mega-projects sponsored by federal funds. In the 1990s, this process was intensified by implementing grain-oriented agriculture projects, where soybean played a key role as the principal commodity for exportation in the region (AGUIAR; MONTEIRO, 2005; BRASIL, 2009). Given the anthropic pressure of the novel extensive agriculture fields over the natural environments of the Piauí Cerrado area, it is imperative to produce multi-temporal geospatial records to support research and the formulation of public policies related to land use and cover in the region.

Thus, mapping from satellite images is one of the most vital data sources to register and investigate the Earth's surface (JENSEN, 2009). The historical series of the LANDSAT satellite is the longest and complete record of continental surface imagery obtained from space since the 1970s (ROY et al., 2014). The availability of LANDSAT images allows conducting studies on different types of land use and cover on different dates, making this program a pivotal instrument to support the investigations about global land changes (NOVO, 2010). Nevertheless, the most important rule for multi-temporal data analysis is the geometric fitness among the layers or images combined to perform the analytical approach (BEUCHLE et al., 2015). Thus, different images must fit each other perfectly to detect changes computed from simple differences between the digital numbers associated with the pixels between two or more scenes (BYRNE et al., 1980).

Broadly sense, image classification is the procedure used to detect the geographic features of interest present in a scene to create a thematic map-like representation. Contrary to the manual feature extraction, the image classification techniques compute a large amount of data and comprehensive geographic coverage within a time-consuming intangible for human operation (MANFRE et al., 2016). Due to a large amount of data and repetitive operations, remote sensing practitioners develop protocols to optimize the procedures (NOBREGA et al., 2010). Therefore, it is easier to adjust the parameters of a given protocol to be applied in a new image dataset than start over a new set of commands and rules from scratch. Among the diversity of image classification techniques, we choose the Geographic Object-Based Image Classification (GeOBIA) (BLASCHKE, 2010) as the primary procedure used in the present investigation. Recent application of OBIA in Cerrado, as shown in Cunha et al. (2020) and Bueno et al. (2019), demonstrate the power of the method for multitemporal image analysis.

Despite the expansion of agriculture and reduction of natural woodland savanna, we hypothesize that not all savanna areas have been reduced within the study area. Thus, we estimate that patches of parkland-grassland-type have increased along the last three decades due to the nature of the grain-oriented agriculture fields (large flat areas) that drives, on the other hand, the reduction of traditional family-based cattle farms. Consequently, this paper addresses the implementation of a replicable model for building a multitemporal land cover dataset in a Cerrado area in the state of Piauí-Brazil using robust approaches for automatic registration and classification of Landsat images. The framework built analytical capacity for assessing and quantifying three decades of landcover changes in the study area, investigating the dynamics of the agriculture use and savanna cover within the period.

2 STUDY AREA AND MATERIAL

2.1 The study area

The area covered by this study involves seven cities in the south of Piauí (Figure 1), located within the region of occurrence of the Cerrado (Brazilian Savanna) biome. Together, these cities have a total of 75,932 inhabitants distributed in an area of 36,134,567 km² (IBGE, 2010).

Figure 1 - The map illustrating the seven municipalities and Landsat scenes used in the investigation.

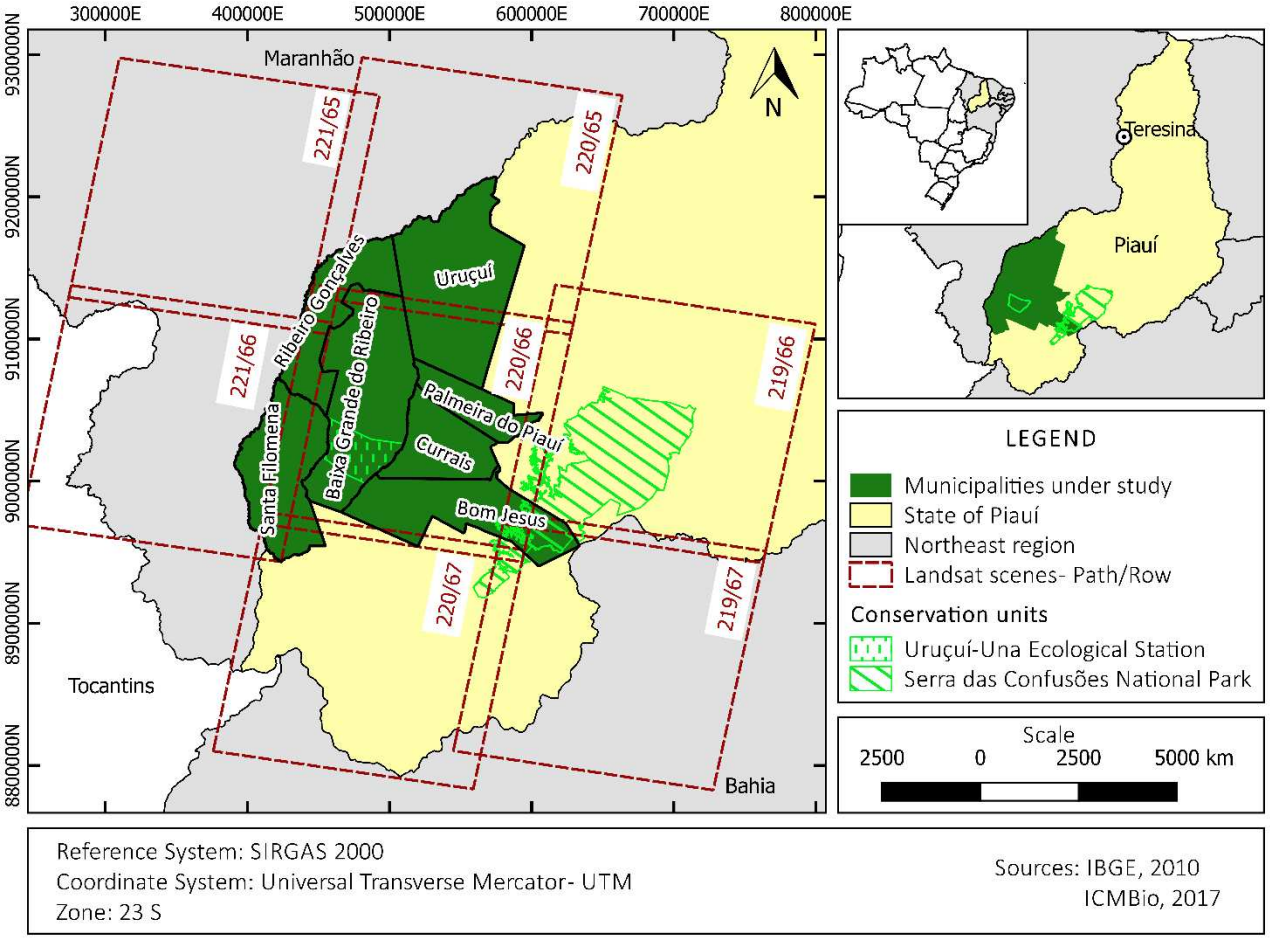

Source: The authors (2021).

According to the Monitoring data of the Cerrado biome for the period 2009-2010 (BRAZIL, 2011b), the seven cities involved in this present high deforestation rates in the state and two of them, Baixa Grande do Ribeiro and Uruçuí, were among the top ten cities that deforested the Cerrado in the whole country for 2002-2011 (BRAZIL, 2009, 2011a, 2011b, 2015). Notwithstanding, these two cities stand at the top of the list of those who deforested the Cerrado in Brazil.

Based on the Mapping of Deforestation records in the Brazilian Biomes by Satellite produced by the MMA in 2009-2010 (BRAZIL, 2011b), a list of priority municipalities was created for ranking conservation actions of the Cerrado biome (PP Cerrado 97/2012). The criteria used to prioritize actions in these cities were: the geographic extension of native vegetation cover, the relevance of the area for biodiversity conservation, and the concentration of extreme poverty in rural areas. Six out of the seven cities in our study area are included in this list.

2.2 The image database and tools

We targeted a timeframe of the past 30 years to assess the metrics of the landcover changes. Thus, we looked ahead three decades, from 1986 as a time zero and using 1996, 2006, and 2016, respectively, as suggested in Cunha et al. (2020). Despite the release of the MapBiomas dataset, a country-wide project of land cover products for Brazil (MAPBIOMAS, 2018), its use was pending validation of local parameters. The need for an accurate classification capable of capturing the landscape's local characteristics (a natural mosaic of flat plateaus and valleys covered by agriculture fields and natural savanna vegetation) encouraged us to avoid traditional per-pixel classification methods, therefore exploring a robust image classification technique with local ground truth validation.

The whole study area is covered by seven Landsat scenes (219/066, 219/067, 220/065, 220/066, 220/067, 221/65, 221/66, see Figure 1). Thus, the investigation gathered 28 full Landsat scenes, where 3/4

correspond to TM Landsat-5, and 1/4 correspond to OLI Landsat-8 images. These images enable to development of multitemporal analysis, capturing the major and minor changes in land cover patterns within the area. The processing relied on Landsat's original ground sample distance of 30 meters. The high spectral correspondence between TM and OLI sensors bands, with the perfect fit in the visible and mid-infrared and partial fit in the near and short infrared bands. These characteristics gave us the confidence to operate images of both sensors in the present investigation. All images used are chargeless and free available at the Brazilian National Institute of Space Research (INPE) and Unites States Geological Service (USGS).

To promote the best use of different solutions, the methodological approach stood on: (i) Remote sensing tools for processing the data, visualizing and analyzing the results, (ii) Geographic Object-Based Image Analysis package for classifying the multi-temporal dataset, and (iv) Landscape ecology toolkit for analyzing and quantifying the landscape metrics of the land cover classes in different years. Thus, the investigation used the following solutions: (i) the ITT image analysis software ENVI version 4.7, (iii) the Trimble eCognition version 9.3, and (ii and iv) the free and open-source Geographic Information System QGIS version 2.18.

3 METHODOLOGICAL APPROACH

In this work, we proposed a robust protocol for mapping the land cover from multitemporal satellite images. In short, the approach consists of [1] Image registration, [2] mosaicking and image preparation, [3] OBIA, and [4] analysis of results. The executed procedures are detailed in the following flowchart (Figure 2).

Figure 2 - General flowchart of the proposed methodology: Image registration [red]; mosaicking and image preparation [yellow]; OBIA [blue]; and analysis of results [green].

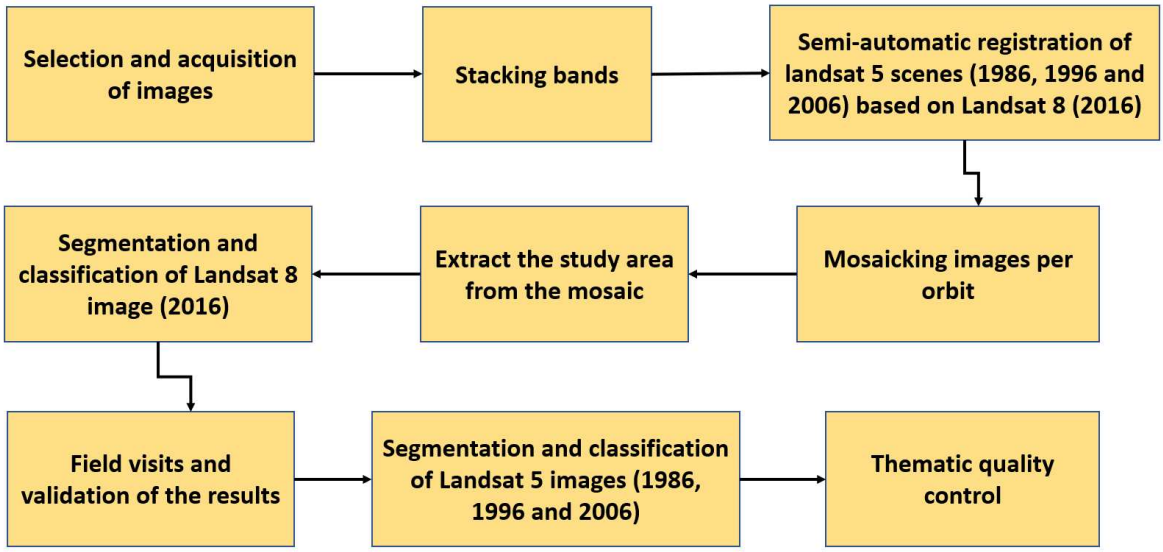

Source: The authors (2021).

3.1 Image Preparation

Data gathering was the first step in the process. The scenes were available per spectral band. Thus after downloading the data, we selected six bands (Blue, Green, Red, Near Infrared, Shortwave Infrared 1 and 2) to be integrated into a multispectral image. The layer stack followed a sequential order to produce one multispectral image per scene per date (28 multispectral images in total). Besides simple, this is a crucial procedure towards automating the process. Any disturbance in the stacking order can compromise the next steps of the methodological approach.

Notwithstanding, the remote sensing images are susceptible to geometric distortions that compromise the positioning accuracy (BENTOUTOU et al., 2005; CRÓSTA, 1992). Traditionally, different techniques are used to minimize or fix the geometric inconsistencies of the image, such as image registration that is a fundamental procedure used to match two or more images taken at different times, from different sensors, or different viewpoints (BERTUCINI JUNIOR; CENTENO, 2016; BROWN, 1992). Next, the multispectral images were accurately registered to avoid geometric inconsistencies among the land cover maps that will be

produced. Finally, the geometric quality of the OLI Landsat-8 images due to the orthorectification process performed by the United States Geological Service (USGS) allows these images to serve as a reference for further registration of other images.

Thus, we established the set of Landsat 8 images (the reference year 2016) as the geometric basis for registering the images of the previous decades. The automatic image registration approach identified homologous points in target images considering a seed point in the reference image and the search window. The core process is based on a convolution window and image correlation process (FARIA, 2017). Besides some GIS and remote sensing software presents an automatic image registration approach built on the toolkit, the solution is not popular among the users, which encouraged us to use it in the present work. The automatic image registration was computed using ENVI software. The tool launches a collection of seed points in the reference image and uses search windows and a convolution process to identify the homologous points in the other images. The highest correlation gives the exact location of the point among the two images. Then, one by one, the seven multispectral images of 2006 were automatically registered to the correspondent image of 2016. Next, the procedure was repeated to the images of 1996 and 1986.

After registering the images based on the Landsat 8 satellite scenes, we create a single raster dataset per year from multiple scenes by mosaicking them, producing four datasets to 2016, 2006, 1996, and 1986, respectively. Due to the geographic amplitude of the study area and the radiometric inconsistencies among the images with specific dates of acquisition, the mosaic requested a strategic radiometric balancing to maximize the quality of the output (NOBREGA; QUINTANILHA, 2004). So, the mosaic was performed per orbit, and the images used correspond to the period between June and August (Frame 1), a few months after the rainy season in the study region. The mosaics were computed using Georeferenced Mosaic tool on ENVI software for the path/rows 219/66, 219/67, 220/65, 220/66, 220/67, 221/65, and 221/66 per year (1986, 1996, 2006 and 2016). We fixed the scenes 220/66 due to the central position among and most prominent in the set, consequently, the other scenes were adjusted to match the reference one. Moreover, the adjustment was set to the entire image instead of an overlapping area. The seamline for mosaicking was 200 pixels, which avoided scars and promoted undetectable mosaicking lines. Furthermore, to speed up the process and optimize the quality of the mosaic, avoiding the pixels external to the limiting polygon, the mosaicking process was computed within the study area only.

Frame 1 – Dates of the images used.

		Path-Row						
		219-66	219-67	220-65	220-66	220-67	221-65	221-66
Year	1986	July/21	July/21	June/10	June/26	June/26	June/17	June/17
	1996	June/30	June/30	June/21	June/21	June/21	June/28	June/28
	2006	July/12	July/12	July/19	July/19	July/19	June/24	June/24
	2016	August/09	August/09	August/08	July/22	July/22	July/08	August/09

Source: The authors (2021).

3.2 Protocolling and Validating OBIA's Approach

The key step towards the successful classification using OBIA is the appropriate segmentation of the image. Thus, the literature provided a background for the shape, compactness, scale, and band weights (FEIZIZADEH et al., 2017; WEZYK et al., 2016). In order to achieve the OBIA classification rule set and a landcover map capable of validation, OBIA was developed solely to the images of the year 2016 (Landsat 8), adapted, and then applied backward to 2006, 1996, and 1986 georegistered images, respectively. The approach allowed a comprehensive evaluation of the classification process, followed by a rigorous ground survey to assess the accuracy of the land cover map produced.

The investigation relied on the traditional typology of land cover classes, such as (Figure 3):

- Developed areas: urban areas, built-up areas, and roads;
- Agricultural fields: crops and artificial pastures;
- Water bodies: rivers, ponds, and dams;
- Woodland savanna: dense shrubs and trees, riparian forests, and dry forest;
- Parkland / Grassland savanna: grass and ground vegetation, wetland, rocky field, palm tree.

Figure 3 - Examples of the landcover classes present in the study area: (1) water body – Parnaíba River, (2) Agriculture field, (3) Woodland savanna, and (4) Parkland / Grassland savanna.

Source: The authors (2021).

The geographic objects resulting from the segmentation were selected and used as samples in the training process. We adopted fuzzy logic as the key strategy for the classification process to minimize the spectral confusion of the classes. After collecting and computing the statistics of the spectral patterns of the samples, the geometric-based metrics were added to the ruleset of the classes for straightening the classification process.

In theory, a classification result with 100% accuracy means that all the images' pixels are assigned to the correct class, thus neither false positives (commission error) nor false-negatives (omission error) exist (CONGALTON; GREEN, 1999). However, the accuracy depends on several factors such as terrain complexity, spatial and spectral resolutions of the sensor system, the classification algorithm, the quality and representativity of the samples, and the complexity of the legend classes (MENESES; ALMEIDA, 2012). Traditionally, remote sensing relies on a discrete multivariate technique called Kappa analysis to assess the classification results accurately. Kappa is a metric based on the difference between the remote sensing classification and the actual reference data, organized in a matrix framework (CONGALTON; GREEN, 1999). Besides the global metric, the matrix-based framework also allows assessing metrics for false-positive (commission error) and false-negative (omission error) per class.

Thus, as for the accuracy assessment of the classification process, one of the challenges was to assure the high thematic quality across the entire study areas even the seven municipalities present isolated and remote areas that are difficult for the perfect distribution of the ground truth samples. Therefore, we selected 154 ground surveyed samples spatially distributed without concentration, which allowed the samples to be collected in the best feasible areas close to the preliminary plan.

3.3 Multitemporal Image Classification

After completing and attesting the classification of 2016 data, an analogous OBIA approach was performed to the other three datasets (2006, 1996, and 1886). Minor adjustments in the segmentation settings were necessary to fit segments to actual geographic objects present in the landscape. This was also evidenced in the classification rules to the previous years of 1986 and 1996, a period in the early stage of the grain-oriented agriculture activities in the region. Samples were pulled up from the images of 1986, 1996, and 2006 and analyzed using visual inspection like the approach used through the validation process in the field.

4 RESULTS AND ANALYSIS

4.1 Automatic Image Registration and mosaicking

Given the availability of orthorectified Landsat 8 images, we used the 2016 scenes as reference for registering the Landsat 5 scenes acquired on previous dates. The automatic registration approach employed up to 200 seed points homogeneously distributed per scene. The threshold for acceptance of the correlation was 90%, so only the homologous points highly correlated to the seed points within the 100x100 pixels window search area were considered anchor points to the image registration.

In order to guarantee the reliability of the registration, all the remaining seed points and the respective homologous points were visually inspected to attest matching and correct positioning. Points with no conformity, i.e., points positioned in areas with no correspondence due to wrong location or abrupt change in landcover pattern, were excluded, and if necessary, new points were added manually. Because of the abundance of the automatic seed points, adding points was necessary only in areas where the low density was detected. After this verification, the procedure was performed with the minimum number of 100 homologous points in each analyzed scene (Figure 4).

Figure 4 - Example of seed points of the 2016 image (left) and homologous points found in 1986 used in the automatic image registration process.

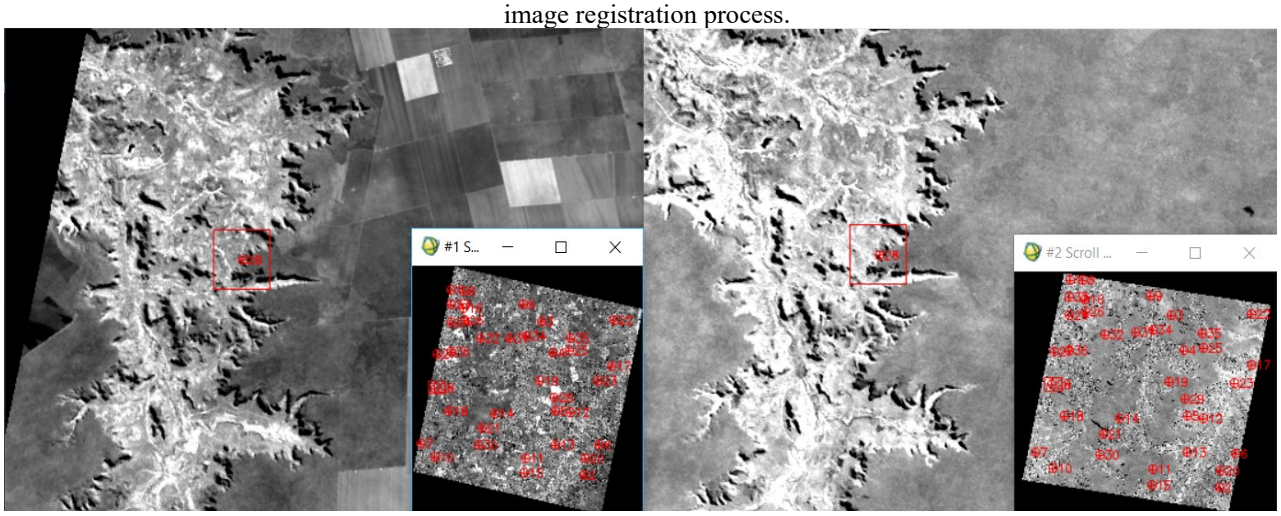

Source: The authors (2021).

All 21 scenes of the Landsat 5 referent to 2006, 1996, and 1986 go through the registration process using the correspondent orthorectified 2016 Landsat 8 scenes. After the registration was completed, the images were loaded together in a GIS framework (i.e., QGIS) for visual inspection. Findings show a perfect geometric fitting between the scenes regarding the natural features such as rivers, cliffs, roads, and other anthropogenic features.

Next, given the database of geographically correlated images of each year studied, the mosaic of the scenes and the land use and cover classification per orbit were executed. The strategy of mosaicking adjacent images per orbit improved the product's quality and sped up the segmentation/classification processes, except in cases where excessive differences in atmospheric conditions were detected. Thus, the approach promoted high-quality mosaics for the further classification process.

4.2 The OBIA Protocol

4.2.1 SEGMENTATION

The segmentation process of Landsat 8 images (Figure 5) was performed using multi-resolution algorithm segmentation of the program eCognition 9.3. For this step we set a scale parameter equal to 100, and the bands 2, 3, 4, 5, 6, and 7 (Landsat 8). The shape and compactness of the segments were set as 0.3 and 0.8, respectivelly, parameters that allowed to capture both anthropogenic agriculture fields and natural features such as dense vegetation along the rivers and valleys. The scale parameter defines the size of the segments to be generated; that is, the larger the value, the larger the size of the segments (SILVA et al., 2016), and consequently, the less the level of detail. Shape and compactness are auxiliary parameters for tunning the strategy based on the digital number of the pixels within the segments to allow flexibility to create the segments' geometry (NOBREGA et al., 2008). All these introduced parameters were defined from several segmentation attempts over the dataset.

For the segmentation of Landsat 5 images, bands 1, 2, 3, 4, 5, and 7 were used. However, adjustments were necessary for the process to end up with segments geometrically compatible with the segments resulting from Landsat 8 data. So, we set 40 for the scale parameter, 0.1 for the shape, and 0.3 for the compactness. According to tests performed with the assignment of several parameters, these parameters best fit the images of the Landsat 5 satellite for the study area. Furthermore, the difference in segmentation parameters between the images of the two Landsat satellites is justified by the difference of sensors (TM and OLI). Therefore, in the images of Landsat 5 satellite, it was necessary to create segments with different parameters to distinguish the mapped targets.

Figure 5 - (1) Landsat 8 image segmentation; (2) Landsat 5 image segmentation.

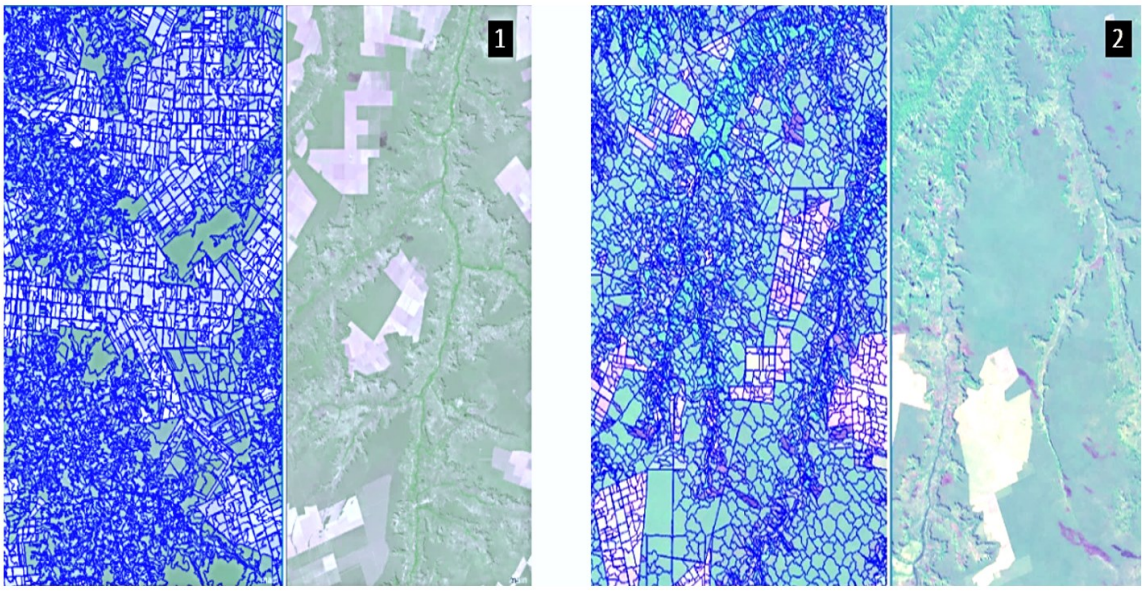

Source: The authors (2021).

4.2.2 SEGMENT SAMPLING

After completing the segmentation, we created the classes and the respective ruleset for each class by sampling the segments and assessing their spectral and geometric parameters. The knowledge from previous fieldwork was essential to promote the correct association between the land use and cover classes seen in the 2016 images and the field. For each class, samples were distributed throughout the region to be classified, obtaining at least 20 samples per class (Figure 6). Then, we collected 50 examples for the vegetation and agricultural activities because these classes are the most expressive in the area.

4.2.3 CLASSIFICATION OF LANDSAT IMAGES

Supervised land use and cover mapping of Landsat images were performed using the classification algorithm. These covered classes were "water bodies", "Agriculture field", “Woodland savanna”, and “Parkland / Grassland savanna”. The urban areas were manually defined by using the image objects resulting from the segmentation process. Because the developed areas are small and in few numbers within the study area, the samples used to assign the class completed the urban areas. In practice, the urban areas were masked out to the classification process, therefore avoiding the typical confusion with other classes.

Figure 6 - Segment samples per class.

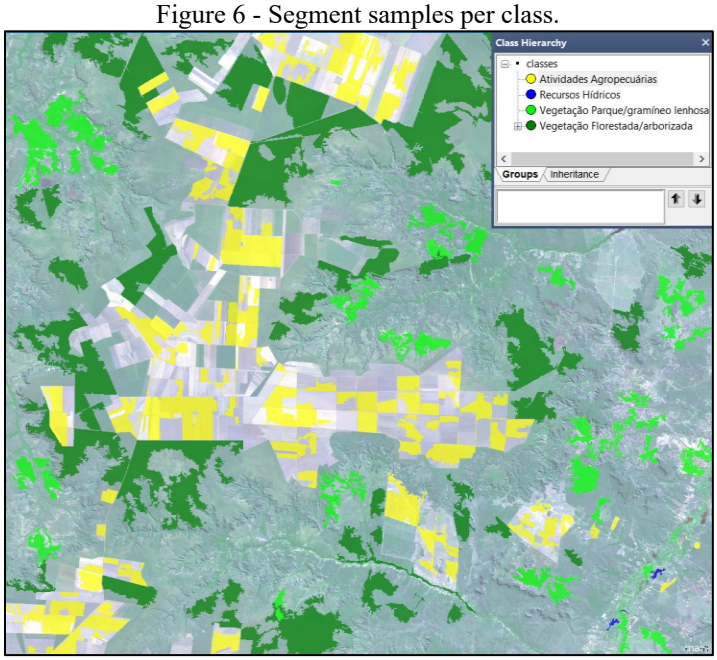

Source: The authors (2021).

4.2.4 PERTINENCE FUNCTIONS USED IN DECISION RULES (FUZZY LOGIC)

For the image classification, the "Nearest Neighbor" method was used, taking, as a rule, the use of the mean value of the segment pixels. Then, by computing the samples, the thresholds were generated for each class (Table 1). All the bands used were considered with equal weights in the classification in this process.

Table 1 - Classification thresholds.

Class	**Pertinence function**	**Thresholds**
Water Bodies	Area	1 / 2,515
	Brightness	30 / 9,465
	Border length	4 / 2,914
	GLCM homogeneity (all directions)	0.004 / 0.30
Agriculture Fields	Area	1 / 147,774
	Brightness	2,134 / 23,103
	Border length	4 / 80,410
	GLCM homogeneity (all directions)	0.2 / 0.78
Parkland / Grassland Savanna	Area	2 / 1,480,490
	Brightness	5,929 / 15,353
	Border length	6 / 241,698
	GLCM homogeneity (all directions)	0.0005 / 0.29
	Rel. Border to Agriculture	0 / 1
Woodland Savanna	Area	9 / 3,079,350
	Brightness	8,667 / 12,372
	Border length	16 / 3,066
	GLCM homogeneity (all directions)	0.0031 / 0.12
	Rel. Border to Agriculture	0 / 1

Source: The authors (2021).

The assigned assignment algorithm was used to refine the classification obtained through decision rules (reclassification) with the already classified images. So, we reclassify the dataset by analyzing metrics such as homogeneity, texture, and edge contact with other classes. The rules used were:

1. Agriculture class with GLCM Homogeneity (all dir.) < 0.2 at level 1: Parkland/Grassland Savanna;
2. Parkland/Grassland Savanna with Rel. border to Agriculture >= 0.47 at level 1: Agriculture;
3. Water Bodies with GLCM Homogeneity (all dir.) >= 0.94 at level 1: unclassified.

4.3 The Thematic Quality Control

The first classification of images occurred for the year 2016. Field visits occurred in August and September 2017. The approach of taking off points was carried through the whole study area, contemplating the seven studied cities. In possession of the classified map for this year, control points were collected in the field (Figure 7) using a navigation GPS receiver and field photographs for data validation. A total of 154 points were collected involving targets from all classes identified. A confusion matrix was assembled between the classes to calculate the Kappa index to validate the mapping results with the points obtained in the field.

Figure 7 - Control points used in the classification validation.

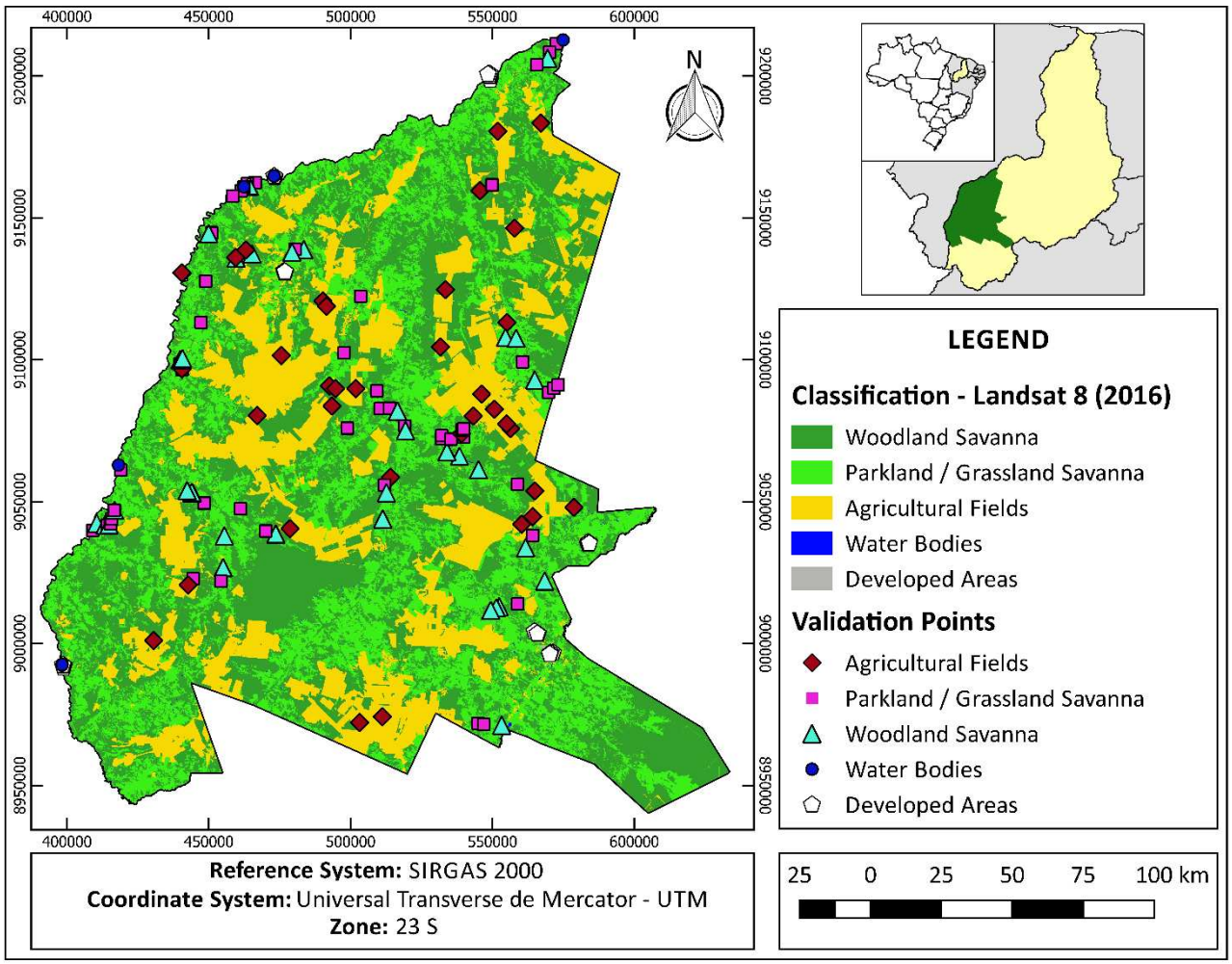

Source: The authors (2021).

4.3.1 KAPPA INDEX AND ERRORS OF COMMISSION AND OMISSION OF CLASSES

Findings of the kappa index for the classification year 2016 was 0.82, considered excellent (K> 0.8) by Congalton; Green (1999). Although the index result was successful, the "Parkland / Grassland savanna" and "Woodland savanna" classes had produced accuracy and user accuracy slightly below 80%, respectively. This slight increase in errors of commission and omission is justified by the confusion between these two classes of subdivision of vegetation, as explained in Frame 2.

Frame 2 - Matrix of confusion.

		Classification						
		Woodland savanna	**Parkland/ Grassland savanna**	**Agricultural fields**	**Developed areas**	**Water bodies**	**Errors of omission**	**User's accuracy**
Ground truth	**Woodland savanna**	28	9	0	0	0	24%	76%
	Parkland/ Grassland savanna	4	42	3	0	0	14%	86%
	Agricultural fields	0	6	31	0	0	16%	84%
	Developed areas	0	0	0	25	0	0%	100%
	Water bodies	0	0	0	0	6	0%	100%
	Errors of commission	13%	26%	9%	0%	0%		
	Producer's accuracy	88%	74%	91%	100%	100%		

Source: The authors (2021).

4.4 Multitemporal Classification and Data Tabulation

The supervised classification of the images of the two Landsat satellites, even of different sensors, was facilitated for comparison using an object-oriented classification method. Therefore, the procedures were based not only on the spectral response of the pixel but also on geometric and textural contexts to classify the land use and cover classes.

This method provided a greater malleability in interpreting the presented raw data, not being limited only to the spectral response of the targets. At the junction of the data of each orbit, we observed no disagreements among the classifications of the three orbits covered by the study area (Figure 8).

Land use and cover data were qualified for each year analyzed (Table 2). The results show an evident increase of agricultural activities and the reduction of forested and arborized vegetation. Figure 9 illustrates the changes in land cover classes type per decade between 1986 and 2016.

As shown in Figure 9, the area occupied by woodland savanna substantially decreased from 74% in 1986 to 44% in 2016 within the study area. Even worst, the deforestation phenomenon was intensified over the decades. Thus, the 30% of loss in woodland savanna corresponds to the 20% of areas converted in agriculture fields and the almost 10% of area converted in grassland and parkland savanna. The increase of agriculture fields shows that the phenomenon is inversely proportional to the loss of woodland savanna. Moreover, it is important to note that urban areas also increased substantially in the period, however still limited to a small fraction of the study area.

Figure 8 - Classification of land use and land cover in the periods studied.

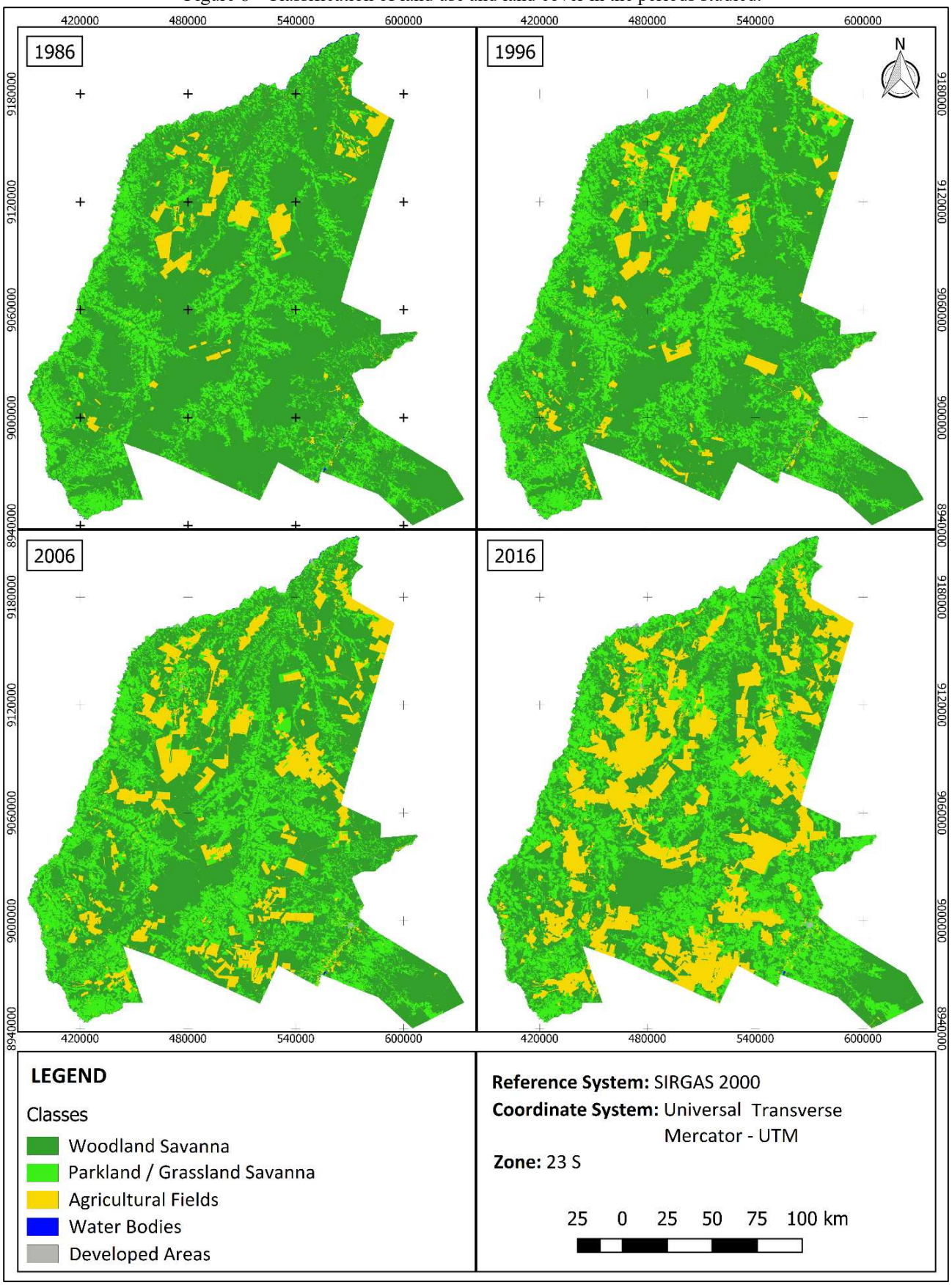

Source: The authors (2021).

Table 2 - Quantitative of areas per class.

Class	Class area (ha)	Percentage
1986		
Woodland savanna	2,663,086.14	73.68%
Agricultural fields	146,060.46	4.04%
Water bodies	2,789.37	0.08%
Developed areas	543.4	0.02%
Parkland savanna / Grassland savanna	802,124.91	22.19%
1996		
Woodland savanna	2,341,521.99	64.78%
Agricultural fields	222,989.22	6.17%
Water bodies	2,144.25	0.06%
Developed areas	959.58	0.03%
Parkland savanna / Grassland savanna	1,046,994.93	28.97%
2006		
Woodland savanna	2,097,910.98	58.04%
Agricultural fields	459,981.09	12.73%
Water bodies	1,885.23	0.05%
Developed areas	1,580.67	0.04%
Parkland savanna / Grassland savanna	1,053,240.84	29.14%
2016		
Woodland savanna	1,579,926.51	43.71%
Agricultural fields	908,447.13	25.13%
Water bodies	2,870.1	0.08%
Developed areas	3,029.49	0.08%
Parkland savanna / Grassland savanna	1,120,330.62	30.99%

Source: The authors (2021).

Figure 9 - Time-series changes on land cover classes per decade between 1986 and 2016.

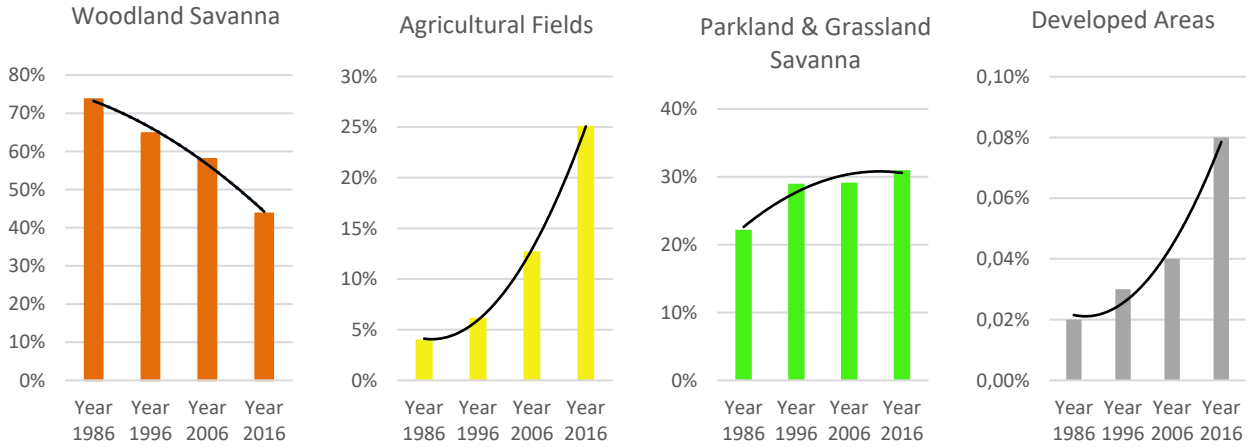

Source: The authors (2021).

5 DISCUSSION AND FUTURE WORK

In this work, we present a method that best suits multi-temporal studies of land use and cover, preprocessing procedures, semi-automatic register, and image classification of the Landsat 5 and 8 satellites were performed, as well as the subsequent validation of the data in the field. This study has become complex because it involves an extensive area encompassing seven Landsat scenes and a 30-year timeframe divided over ten-year periods.

Thus, we present the results of a multi-temporal analysis of Landsat images (PESSOA et al., 2013)

and the results obtained in the Brazilian states of Mato Grosso and Rio de Janeiro. In a study on the register of a series of Landsat images (BERTUCINI JUNIOR; CENTENO, 2016), the process can be automated (FARIA, 2017), and that success depends on the contrast quality of the regions used in the development of this research.

Since this is comparative research between four distinct periods, the work with non-orthorectified orbital images makes the geospatial correspondence between several years of data is impossible. The lack of geometric correspondence does not allow comparing land use and cover evolution in a given area. Another problem in multitemporal studies using different orbital sensors is finding suitable satellite image classification methods that minimize these differences. The use of oriented classification registration and classification using OBIA has proved to be essential tools for solving problems evidenced in multitemporal satellite data. Therefore, this investigation is necessary because it paved a roadmap that can be executed in the other multitemporal analyses of land use and land cover and other themes linked to historical data of a region.

Although, the multitemporal OBIA approach provided a mechanism to support the detection and classification of the land use and cover classes used in this investigation, including the small patches of grassland savanna. It is critical to highlight that the proposed method meets the need of a robust approach capable of mapping minor changes in the landscape, so we can quantify not only the expansion of the agriculture over the savanna but also small patches of savanna that arise in the study area along the last three decades.

6 CONCLUSION

As for the methodology, the proposed approach attested to the efficiency of the semi-automatic image-to-image registration as an effective method for the geometric correction of Landsat scenes. Furthermore, we observed that the techniques used in this multitemporal study provide a correct geographic positioning between the images of all the analyzed years.

The land use and cover classification obtained for the study area was satisfactory during all years covered, even with different sensor images. Therefore, we concluded that the object-based classification procedures are appropriate for multitemporal studies based on the methodologies performed in this work. Based on the confusion matrix and the calculated accuracy, it can be stated that this procedure was able to classify the region correctly in the analyzed period.

Combined, the precise semi-automatic image georegistering and the object-based image classification provided a powerful tool to map land cover changes in critical areas of the Cerrado. In addition, the refined image segmentation allowed to detect patches of parkland savanna and grassland savanna, which deforestation does not match the woodland savanna.

Our findings show a strong reduction of woodland savanna that covered 73% of the study area in 1986 and only 43% in 2016, while agriculture areas were increasing from 4% to 25%. However, the quality of the geometric matching of the multitemporal images and the OBIA classification method allowed us to map minor changes in the landscape. Thus, the hypothesis of small patches of grassland savanna emerging in areas of degraded cattle farms and hills could be proved. The results showed a high increase from 22% in 1986 to nearly 31% in 2016.

Acknowledgments

This research was supported by Conselho Nacional de Desenvolvimento Científico e Tecnológico (CNPq, research productivity grants 309763/2020-7 and 315631/2021-0 to Diego Macedo and Rodrigo Nóbrega), Coordenação de Aperfeiçoamento de Pessoal de Nível Superior (CAPES, Finance Code 001).

Authors' Contribution

The first author (Danilo de Sousa Lopes) was responsible for Conceptualization, Research, Visualization, and Writing – draft. The second author (Rodrigo Affonso de Albuquerque Nóbrega) was responsible for Conceptualization, Supervision and Writing – revision and editing. The third author (Diego Rodrigues Macedo) was responsible for Conceptualization, Supervision and Writing – revision and editing.

Conflict of interest

The authors declare no conflict of interest.

References

AGUIAR, T. J. A.; MONTEIRO, M. S. L. Modelo agrícola e desenvolvimento sustentável: a ocupação do cerrado piauiense. **Ambiente & Sociedade**, v. 8, n. 2, 2005. DOI: 10.1590/S1414-753X2005000200009.

BENTOULOU, Y.; NASREDDINE, T.; KPALMA, K.; RONSIN, J. An automatic image registration for application in remote sensing. **IEEE Transactions on Geosciences and Remote Sensing**, v. 43, n. 9, p. 2127-2137, 2005. DOI: 10.1109/TGRS.2005.853187.

BERTUCINI JUNIOR, J. J.; CENTENO, J. A. S. Registro de Série de Imagens Landsat Usando Correlação e Análise de Relação Espacial. **Boletim de Ciências Geodésicas**, v. 22, n. 4, p. 685-702, 2016. DOI: 10.1590/S1982-21702016000400039.

BEUCHLE, R.; GRECCHI, R. C.; SHIMABUKURO, Y. E.; SELIGER, R.; EVA, H. D.; SANO, E.; ACHARD, F. Land cover changes in the Brazilian Cerrado and Caatinga biomes from 1990 to 2010 based on a systematic remote sensing sampling approach. **Applied Geography**, v. 58, p. 116-127, 2015. DOI: 10.1016/j.apgeog.2015.01.017.

BLASCHKE, T. Object based analysis for remote sensing. **ISPRS Journal of Photogrammetry and Remote Sensing**, v. 65, p. 2-16, 2010. DOI: 10.1016/j.isprsjprs.2009.06.004.

BRAZIL. Ministério do Meio Ambiente – MMA. **Relatório Técnico de Monitoramento do Desmatamento no Bioma Cerrado, 2002 a 2008**: Dados Revisados. 2009. Available at: http://www.mma.gov.br/estruturas/sbf_chm_rbbio/_arquivos/relatorio_tecnico_monitoramento_desmate_bioma_cerrado_csr_rev_72_72.pdfc. Accessed in: 22 Mar. 2018.

BRAZIL. Ministério do Meio Ambiente – MMA. **Monitoramento do Desmatamento nos Biomas Brasileiros por Satélite**. Monitoramento do Bioma Cerrado 2008 a 2009. 2011a. Available at: http://www.mma.gov.br/estruturas/sbf_chm_rbbio/_arquivos/relatoriofinal_cerrado_2008_2009_72.pdf. Acessed in: 22 Mar. 2017.

BRAZIL. Ministério do Meio Ambiente – MMA. **Monitoramento do Desmatamento nos Biomas Brasileiros por Satélite**. Monitoramento do Bioma Cerrado 2009 a 2010. 2011b. Available at: http://www.mma.gov.br/estruturas/sbf_chm_rbbio/_arquivos/relatoriofinal_cerrado_2010_final_72_1.pdf. Acessed in: 22 Mar. 2018.

BRAZIL. Ministério do Meio Ambiente – MMA. **Monitoramento do Desmatamento nos Biomas Brasileiros por Satélite**. Monitoramento do Bioma Cerrado 2010 a 2011. 2015 Available at: http://www.mma.gov.br/images/arquivo/80120/PPCerrado/Relatorio%20Tecnico_Bioma%20Cerrado_2011vfinal.pdf. Acessed in: 22 Mar. 2017.

BROWN, L. G. A survey of image registration techniques. **ACM Computing Survey**, v. 24, n. 4, p. 325-376, 1992. DOI: 10.1145/146370.146374.

BUENO, I. T.; ACERBI JUNIOR, F. W.; SILVEIRA, E. M. O.; MELLO, J. M.; CARVALHO, L. M. T.; GOMIDE, L. R.; WITHLEY, K.; SCOLFORO, J. S. Object-Based Change Detection in the Cerrado Biome Using Landsat Time Series. **Remote Sensing**, v. 11, n. 570, 2019. DOI: 10.3390/rs11050570.

BYRNE, G. F.; CRAPPER, P. F.; MAYO, K. K. Monitoring land-cover change by principal component analysis of multitemporal landsat data. **Remote Sensing of Environment**, v. 10 n. 3, p. 175-184, 1980. DOI: 10.1016/0034-4257(80)90021-8.

CONGALTON, R.G.; GREEN, K. **Assessing the accuracy of remotely sensed data**: principles and practices. New York: Lewis Publishers, 1999. 137p.

CRÓSTA, A. P. **Processamento Digital de Imagens de Sensoriamento Remoto**. Campinas, SP: IG/UNICAMP, 1992.

CUNHA, E. R.; SANTOS, C. A. G.; SILVA, R. M.; BACANI, V. M.; TEODORO, P. E.; PANACHUKI, E.; OLIVEIRA, N. S. Mapping LULC types in the Cerrado-Atlantic Forest ecotone region using a Landsat time series and object-based image approach: A case study of the Prata River Basin, Mato Grosso do Sul, Brazil. **Environmental Monitoring and Assessment**, v. 192, n. 2, article n. 136, 2020. DOI: 10.1007/s10661-020-8093-9.

FARIA, T. **Classificação em área urbana apoiada em imagens aéreas e dados LIDAR**. Dissertação de Mestrado. Programa de Pós Graduação em Análise e Modelagem de Sistemas Ambientais, Instituto de Geociências, Universidade Federal de Minas Gerais, Belo Horizonte, MG, 2017. 94p. Available at: http://www.bibliotecadigital.ufmg.br/dspace/handle/1843/IGCM-AQXN63. Accessed in: 01 March 2019.

FEIZIZADEH, B.; BLASCHKE, T.; TIEDE, D.; MOGHADDAM, M.H.R. Evaluating fuzzy operators of an object-based image analysis for detecting landslides and their changes. **Geomorphology**, v. 293, part A, p. 240-254, 2017. DOI: 10.1016/j.geomorph.2017.06.002.

IBGE. Instituto Brasileiro de Geografia e Estatística. **Censo Demográfico de 2010**. Características da população e dos domicílios: resultados do universo. Rio de Janeiro, 2010.

JENSEN, J. R. **Sensoriamento remoto do ambiente**: Uma perspectiva em recursos terrestres. 2ed. São José dos Campos, SP: Parêntese, 2009.

MANFRE, L. A.; NOBREGA, R. A. A.; QUINTANILHA, J. A. Evaluation of Multiple Classifier Systems for Landslide Identification in LANDSAT Thematic Mapper (TM) Images. **ISPRS International Journal of Geo-Information**, v. 5, p. 164, 2016. DOI: 10.3390/ijgi5090164.

MENESES, P. R.; ALMEIDA, T. (org.) **Introdução ao Processamento de Imagens de Sensoriamento Remoto**. Brasília.DF: CNPq, 2012.

MAPBIOMAS. **Projeto de Mapeamento Anual da Cobertura e Uso do Solo do Brasil**. 2018. Available at: https://mapbiomas.org. Acessed in: 29 Nov. 2018.

NOBREGA, R. A. A.; AANSTOOS, J.; DABBIRU, L. An innovative approach to aid the detection of anomalies along the Mississippi Levees by bridging SAR and GIS. In: 2010 Geospatial Conference, 2010, Athens. **Proceedings of 2010 Geospatial Conference**, 2010.

NOBREGA, R. A. A.; QUINTANILHA, J. A. Comparative analysis of automatic digital image balancing and standard histogram enhancement techniques in remote sensing imagery. **Revista Brasileira de Cartografia**, v. 56, n. 1, p. 55-64, 2004. Available at: https://seer.ufu.br/index.php/revistabrasileiracartografia/article/view/43502. Accessed in: 18 Jan. 2022.

NOBREGA, R. A. A.; O´HARA, C. G.; QUINTANILHA, J. A. An object-based approach to mine roads features over informal settlements in Sao Paulo city. In: Blascke, T. ; Lang, S.; Hay, G. **Object-based image analysis.** 1st ed., Berlin, Springer-Verlag, p. 597-613, 2008.

NOVO, E. M. L. M. **Sensoriamento Remoto:** Princípios e Aplicações. 4 ed., São Paulo, SP: Blucher, 2010.

PESSOA, S. P. M.; GALVANIN, E. A. S.; KREITLOW, J. P.; NEVES, S. M. A. S.; NUNES, J. R. S.; ZAGO, B. W. Análise espaço-temporal da cobertura vegetal e uso da terra na interbacia do rio Paraguai médio-MT, Brasil. **Revista Árvore**, v. 37, n. 1, 2013. DOI: 10.1590/S0100-67622013000100013.

ROY, D.; WULDER, M. A.; LOVELAND, T. R.; WOODCOCK, C. E.; ALLEN, R. G.; ANDERSON, M. C.; HELDER, D.; IRONS, J. R.; JOHNSON, D. M.; KENNEDY, R.; SCANBOS, T. A. SCHAAF, C. B.; SCHOTT, J. R.; SHENG, Y.; VERMOTE, E.F.; BELWARD, A. S.; BINDSCHADLER, R.; COHEN, W. B.; GAO, F.; HIPPLE, J. D.; HOSTERT, P.; HUNTINGTON, J.; JUSTICE, C. O.; KILIC, A.; KOVALSKYY, V.; LEE, Z. P.; LYMBURNER, L.; MASEK, J. G.; MCCORKEL, J.; SHUAI, Y.; TREZZA, R.; VOGELMANN, J.; WYNNE, R. H.; ZHU, Z. Landsat-8: Science and product vision for terrestrial global change research, **Remote Sensing of Environment**, v. 145, p. 154-172, 2014. DOI: 10.1016/j.rse.2014.02.001.

SILVA, A. A.; OLIVEIRA, A. P. G.; PARANHOS FILHO, A. C.; GROGIO, A. M. **Uso do eCognition 8 para classificação de imagem de satélite com alta resolução**. Mossoró, RN: EDUERN. 2016.

STRASSBURG, B. B. N.; BROOKS, T.; FELTRAN-BARBIERI, R.; IRIBARREM, A.; CROUZEILLES, R.;

LOYOLA, R.; LATAWIEC, A. E.; OLIVEIRA FILHO, F. J. B.; SCARAMUZZA, C. A. M.; SCARANO, F. R.; SOARES-FILHO, B.; BALMFORD, A. Moment of truth for the Cerrado hotspot. Nature Ecology & Evolution, v. 1, article n. 99. 2017. DOI: 10.1038/s41559-017-0099.

WEZYK, P.; HAWRYLO, P.; SZOSTAK, M.; PIERZCHALSKI, M.; KOK, R. Using Geobia and Data Fusion Approach for Land Use and Land Cover Mapping. **Quaestiones Geographicae**, v. 35, n. 1, p. 93-104, 2016. DOI: 10.1515/quageo-2016-0009.

Biography

Danilo de Sousa Lopes was born in 1990 in Teresina - Piaui, Brazil. He holds a bachelor's degree in Environmental Management and Geoprocessing from the Federal Institute of Piauí (IFPI), and a master's degree in Analysis and Modeling of Environmental Systems from the Federal University of Minas Gerais (UFMG). Danilo currently works at the Center for Land and Environmental Geotechnology of the State of Piauí (CGEO) and develops activities involving the National Rural Environmental Registry, land tenure regularization, and object-based image classification techniques, applied to environmental mapping/use and land cover.